Thin-Walled Structures 47 (2009) 1059–1068

Contents lists available at ScienceDirect

Thin-Walled Structures

journal homepage: www.elsevier.com/locate/tws

# Experimental study on repair of fatigue cracks at welded web gusset joint using CFRP strips

Hitoshi Nakamura [a,*], Wei Jiang [a], Hiroyuki Suzuki [b], Ken-ichi Maeda [a], Takao Irube [c]

[a] Department of Civil and Environmental Engineering, Tokyo Metropolitan University, Japan
[b] Department of Architecture, Meisei University, Japan
[c] TTK Corporation, Japan

ARTICLE INFO

Available online 9 January 2009

*Keywords:*
Carbon fiber reinforced polymer strip
Lamination
Repair
Fatigue crack
Welded joint
Drill-hole

ABSTRACT

This paper presents repair methods of fatigue cracks using CFRP strips. In particular, the subject of repair is fatigue cracks initiated at welded web gusset joints, which are the typical details in steel bridges. Several repair methods were investigated experimentally focusing on weld details. In addition, more effective repair methods were also investigated using combination of CFRP strips and drill-holes. As a result, it was found that fatigue life after repair was significantly improved. Therefore, the authors confirmed the feasibility of the proposed technique as a useful repair method to improve fatigue life of steel structures.



## 1. Introduction

In recent years, reports of fatigue damage to steel bridges have increased in Japan with the increase of vehicle load and volume of traffic [1]. Since fatigue cracks are often initiating in narrow locations, where some members are crossing each other and have complicated details peculiar to welded joints, it is difficult to repair and reinforce them. CFRP is expected to be a useful material for repairing and reinforcement of existing steel structures [2–4], because of its lightweight, high strength and excellent corrosion resistance. In addition, the joint method for CFRP strips is very simple and is also easy to apply on site. Recently, in order to utilize CFRP effectively, many researches have been done on welded connections and fatigue strengthening [5–9].

The fundamental studies have been performed experimentally and analytically using steel flat plates [10,11], and the validity of crack repair has been verified. Aiming at application to real structures, the examination was started in consideration of the welded detail [12,13]. The subject of repair is fatigue cracks initiated at welded web gusset joints, which are the typical details in steel bridges. Therefore, the authors have proposed the practical construction method using CFRP strips to repair fatigue cracks at welded web gusset joints.

This study examined a more suitable repair method, using specimens with out-of-plane welded gusset joints, and fatigue tests were carried out with various bonding methods of CFRP strips and varying the number of laminations. The effects of repair and the progress of fatigue cracks after repair were also considered. Moreover, in order to increase the effectiveness of the repair, CFRP strips were used in combination with drill-holes. A drill-hole is a construction method, also called a stop-hole and is generally applied as a temporary repair method on site. Drill-holes are applied to reduce the stress concentration at the tips of cracks. Several combinations of CFRP strips and drill-holes were investigated by static loading tests and fatigue tests.

## 2. Experimental procedure

### 2.1. Specimens and material properties

The specimen is shown in Fig. 1. It was fabricated with gusset plates ($W100 \times T9 \times L140\,\text{mm}^3$) welded to both sides at the center of the steel plate ($W250 \times T9 \times L1040\,\text{mm}$). The mechanical properties of steel, the CFRP strip, and epoxy resin adhesive are shown in Table 1. The CFRP strip is 1.2 mm in thickness. The carbon fiber is arranged unidirectionally.

In addition, in order to investigate the effects of the bonding methods and the laminations on the bond strength, the tensile shear tests were conducted using double-lap adhesive joints. The specimen is shown in Fig. 2. Its width and thickness are 100 and 9 mm, respectively. It was cut off at the dashed line as shown in Fig. 1(a). The fatigue crack was initiated at the weld toe of the web gusset plate.

* Corresponding author.
*E-mail address:* hnaka@tmu.ac.jp (H. Nakamura).

0263-8231/$ - see front matter © 2008 Elsevier Ltd. All rights reserved.
doi:10.1016/j.tws.2008.10.016

**Nomenclature**

| | |
|---|---|
| $K$ | initial rigidity in linear relation of load–displacement curve |
| $\Delta P$ | incremental applied load |
| $\Delta D$ | incremental displacement |
| $\Delta\sigma_n$ | nominal stress range of steel plate |
| $\sigma$ | longitudinal stress |
| $a$ | crack length |
| $D$ | crack opening displacement |
| $N_f$ | number of cycles from start of fatigue test to failure |
| $N_i$ | number of cycles from start of fatigue test until the crack length reached 15 or 50 mm |
| $N_p$ | number of cycles from restart after repair to failure |

### *2.2. Repair method*

Two series of repair methods using CFRP strips are shown in Fig. 3. The cracked specimens were repaired when the crack progressed to a length of approximately 15 mm (it is equivalent to 12% of the overall width) from the center of the specimen to both side edges by cyclic loading test. The repair methods are described as follows.

#### *2.2.1. Series S*

In series S as shown in Fig. 3(a), four single-layered CFRP strips ($W25 \times T1.2 \times L100$ mm) were simply bonded to both sides of the weld bead in order to reduce the stress concentration at crack tips.

#### *2.2.2. Series M*

First of all, in order to improve the bonding surface, the weld bead was finished using a pencil grinder. The multi-layered CFRP strips ($W50 \times T1.2 \times L200$ mm) with a rectangular slit in the center were bonded close to the weld bead. The single-layered CFRP strip ($W25 \times T1.2 \times L100$ mm) was bonded on both sides. In series M as shown in Fig. 3(b), the number of laminations was considered. The effective repair is expected by the reduction in the crack opening displacement, since the crack opening is perfectly covered with multi-layered CFRP strips. Fig. 4 shows an example of repair method in series M5 with five layers.

The used adhesive hardens at ordinary temperature, and reaches the required bond strength in a day. The specimens were cured at 40 °C for a week after repair, because of elimination of dispersion caused by the curing condition of the adhesive.

## 3. Adhesion performance of double-lap joints considering gusset details

### *3.1. Experimental series and testing procedure*

The experimental series is shown in Table 2. As mentioned above, the repair was performed by the two repair methods as shown in Fig. 5. In series DL-M, the number of laminations was 1, 3, 5 or 7 layers. In series DL-S, the CFRP strip was single-layered, and its length was changed as 100 and 200 mm. The bonding surface was sandblasted. The shear tensile tests were conducted using the universal testing machine with a capacity of 1000 kN. The loading speed is 5 mm/min by displacement control. As shown in Fig. 5 and Photograph 1, strains on CFRP strips and opening displacements at joints were measured using strain gages and crip-type displacement transducers.

### *3.2. Static loading test results*

The relationships between the tensile load $P$ and the opening displacement $D$ at the joint is shown in Fig. 6. All the series show nonlinear behavior from the low level of tensile load. In DL-M5 and DL-M7, the tensile load decreased locally at approximately 200 kN because of the yielding in the narrow section of the grip.

In order to compare the rigidity of the adhesion joint, the initial rigidity $K$ is calculated in the linear relation of the $P$–$D$ curve shown in Fig. 6. The initial rigidity $K$ is defined by the following equation:

$$K = \frac{\Delta P}{\Delta D} \tag{1}$$

where $\Delta P$ and $\Delta D$ are the incremental tensile load and the incremental displacement in the range from 20 to 40 kN. Fig. 7 shows the maximum tensile load $P_{max}$ and the initial rigidity $K$ of all the series. In series DL-S, maximum tensile load increases a little, so that the length of CFRP strips is long. In series DL-M, the

**Table 1**
Mechanical properties of steel, CFRP strip and epoxy resin adhesive.

| | Steel plate (JIS SM400A) | CFRP strip | Epoxy resin adhesive |
|---|---|---|---|
| Yield point (MPa) | 293 | – | – |
| Tensile strength (MPa) | 453 | 2664 | 30 |
| Elongation (%) | 23 | 1.9 | – |
| Elastic modulus (GPa) | 204.5 | 188 | 1.5 |

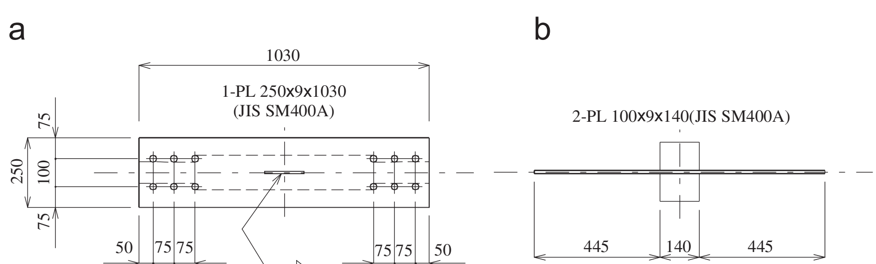


**Fig. 1.** Specimen configuration for fatigue test: (a) plan and (b) elevation.

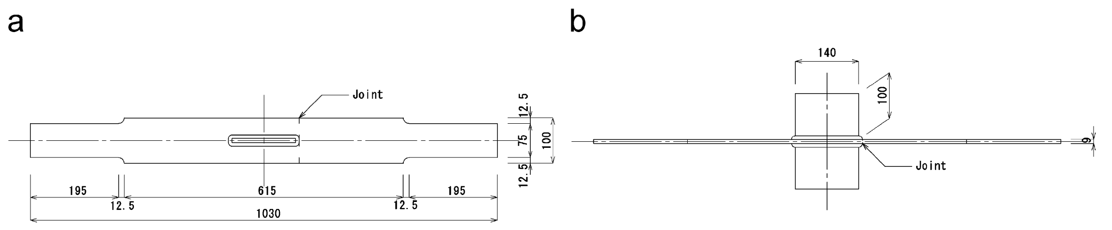


**Fig. 2.** Specimen configuration for double-lap adhesive joints: (a) plan and (b) elevation.

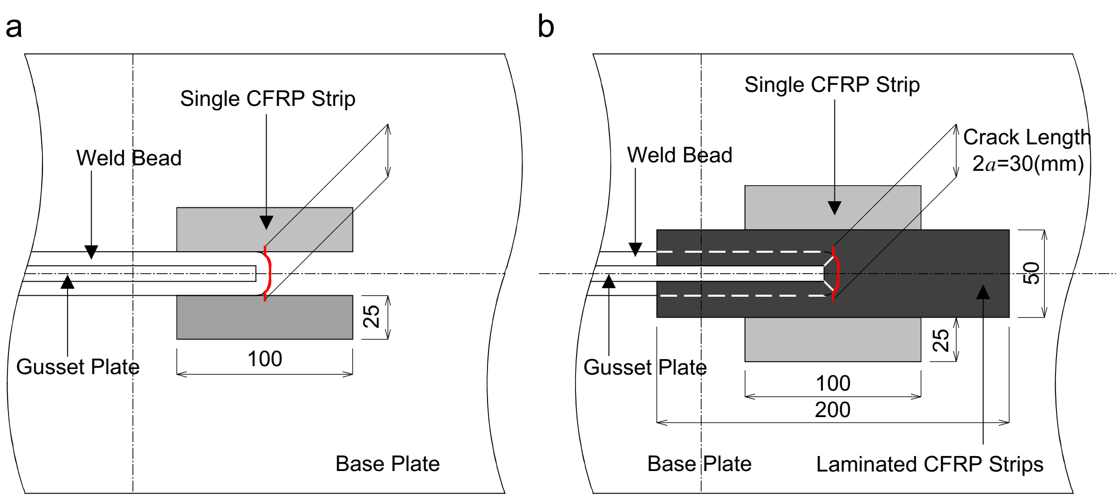


**Fig. 3.** Repair method: (a) series S and (b) series M.

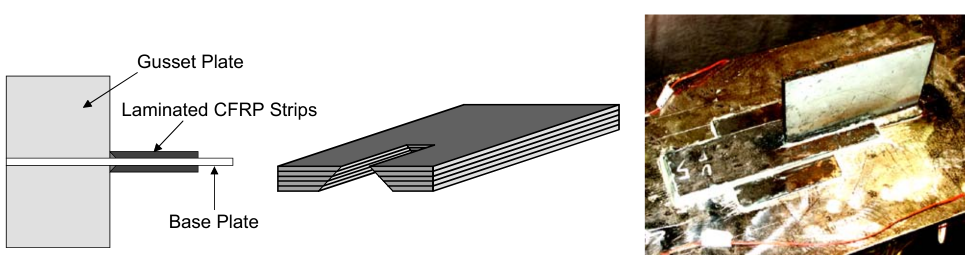


**Fig. 4.** Example of repair method in series M5.

**Table 2**
Experimental series of double-lap adhesive joints.

| Series | Repair method | CFRP strip | |
|---|---|---|---|
| | | Single-layered part (mm) | Multi-layered part |
| DL-S1 | Fig. 5(a) | 100 | – |
| DL-S2 | Fig. 5(a) | 200 | – |
| DL-M1 | Fig. 5(b) | 100 | 1-layer at 200 mm |
| DL-M3 | Fig. 5(b) | 100 | 3-layer at 200 mm |
| DL-M5 | Fig. 5(b) | 100 | 5-layer at 200 mm |
| DL-M7 | Fig. 5(b) | 100 | 7-layer at 200 mm |

maximum tensile load is higher compared with series DL-S, and increasing the number of laminations. Although the initial rigidity $K$ is equivalent in spite of the length of CFRP strips in series DL-S, it

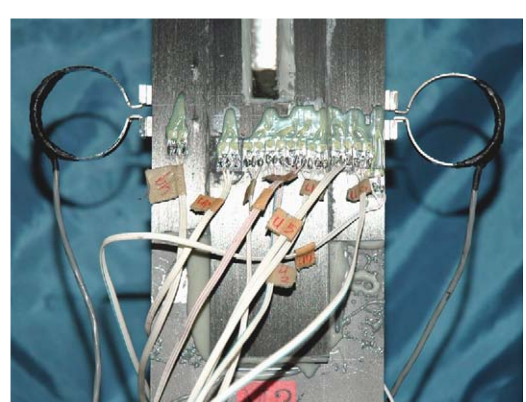


**Photograph 1.** Test setup of series DL-M3.

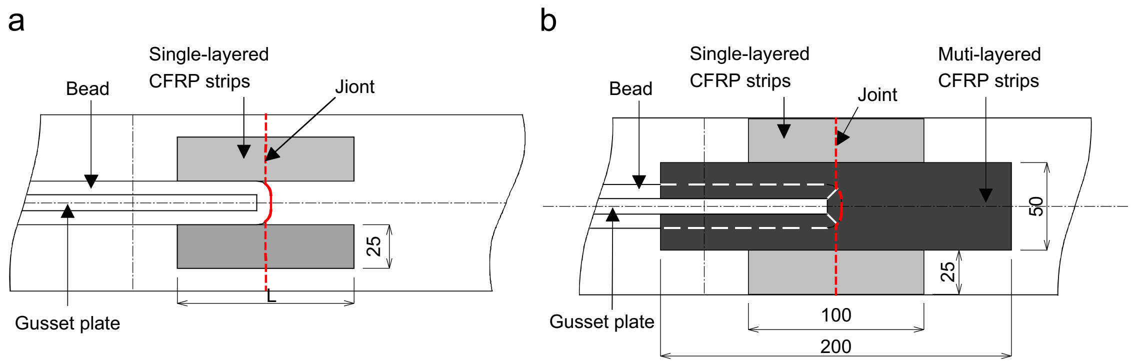


**Fig. 5.** Repair method for double-lap adhesive joints: (a) series DL-S and (b) series DL-M.

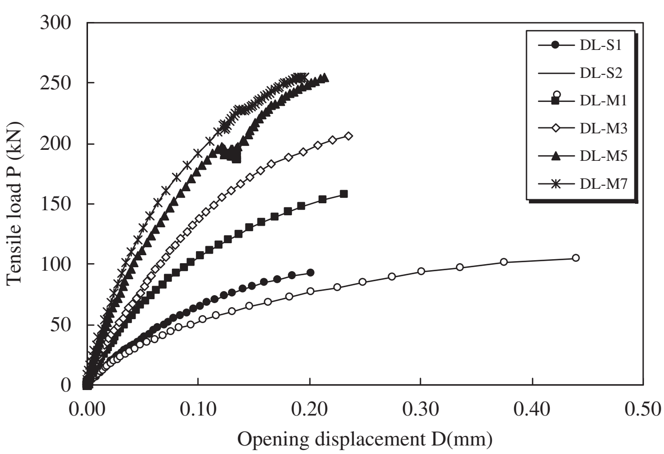


**Fig. 6.** Relationships between tensile load and opening displacements at joint.

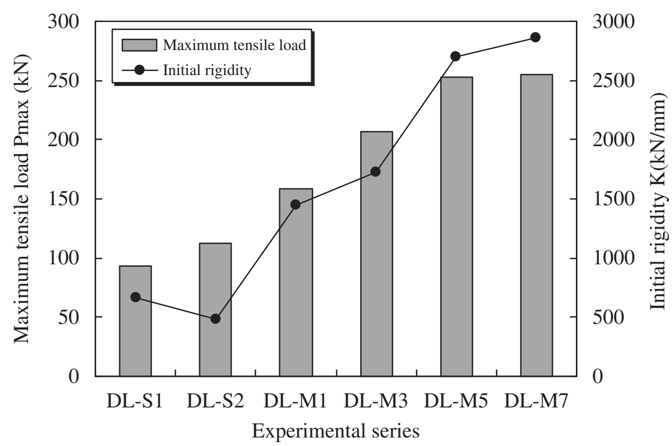


**Fig. 7.** Maximum tensile load and initial rigidity.

is increased with increasing the number of laminations in series DL-M. Since the opening displacement becomes small increasing the initial rigidity, the effective repair can be expected in the case like a crack repair. Consequently, it can be considered that the required number of laminations is five layers regarding upper limits for the maximum tensile load and the initial rigidity.

Fig. 8 shows the relationships between the nominal stress $\sigma_n$ and the tensile stresses on CFRP strips for multi-layered and single-layered parts, respectively. The nominal stress $\sigma_n$ is the value of $P/A$, where $P$ and $A$ are the tensile load and the sectional area of the specimen, respectively. Tensile stresses were averaged for each of the multi-layered and single-layered parts using strain gages on CFRP strips. At the single-layered part of all the series, CFRP strips are subjected to the high tensile stresses of 750–1100 MPa in the ultimate. The stress of the single-layered part becomes small on increasing the number of laminations. It means that CFRP strips of multi-layered part are subjected to large tensile forces. On the other hand, the stress of the multi-layered part becomes lower as the number of laminations increases. From a viewpoint of the sharing force per layer, lamination of CFRP strips is not necessarily rational. However, as mentioned previously, since the lamination gives high rigidity, the effective reinforcement can also be expected in the case aiming at a crack repair.

Finally, an example of the fracture in DL-M7 is shown in Photograph 2. The brittle fracture including the delamination between CFRP strips was observed.

**Photograph 2.** An example of the fracture in series DL-M7.

## 4. Repair effects and fatigue durability

### 4.1. Testing procedure

The loading tests were conducted in order to verify repair effects. Fig. 9 and Photograph 3 show the loading system of the

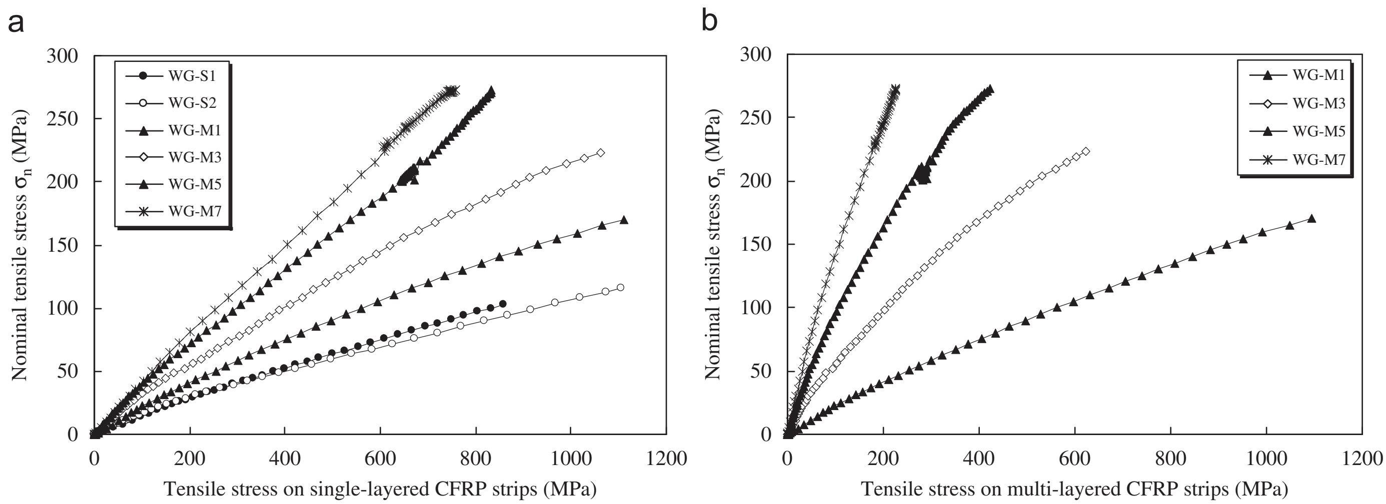


**Fig. 8.** Relationships between nominal stress and tensile stresses on CFRP strips: (a) on single-layered CFRP strips and (b) on multi-layered CFRP strips.

**Photograph 3.** Test setup of loading system.

I-shaped girder and test setup, respectively. The specimen was connected to the loading system with high-strength bolts. The load was applied by four-point bending. The uniform tensile stress was introduced into the specimen according to the uniform bending moment of the bottom flange. An electro-hydraulic servo actuator with a capacity 750 kN was used. In fatigue test, the waveform of the cyclic load was a sine wave with a frequency of 2 Hz. The minimum stress was approximately 20 MPa, and the maximum stress varied according to the nominal stress range $\Delta\sigma_n$ from 64 to 114 MPa. The experimental series is shown in Table 3. In series M, the number of laminations was 1, 3 or 5 layers.

### 4.2. Static loading test results

To begin with, the repair effects under the static loading are described. The cracks were initiated by fatigue test ($\Delta\sigma_n = 100$ MPa), and the simplest repair of series S was performed, when the crack length $a$ reached 55.7 mm (it is equivalent to approximately 45% of the overall). The static loading test was carried out before and after repair. The distribution of longitudinal stress and crack opening displacement in the steel plate were investigated. They were measured using strain gages and clip-type displacement transducers.

In addition, in order to evaluate the validity of experimental results, elasto-plastic finite displacement analysis was carried out with 3D FEA code, Msc. Marc. Fig. 10 shows the analytical model attached to the single-layered CFRP strip. Regarding symmetric boundary condition, only $\frac{1}{4}$ of the specimen was modeled. Same as in the experiment, the tensile stress of 120 MPa was uniformly applied.

As a result of experiment and analysis, the distribution of longitudinal stress and crack opening displacement are shown in Figs. 11 and 12. There is plastic zone by high stress concentration around the crack tip after repair. The longitudinal stresses reduced. The plastic zone decreased after repairing as shown in the analytical model. The crack opening displacements also reduced in general. For example, the crack opening displacement is lowered by about 40% in the center of the specimen. It can be seen that good agreement was achieved between the experimental and analytical results.

### 4.3. Fatigue test results

In order to evaluate fatigue life after repair, the *S–N* diagram was described using the number of cycles from the restart after repair to failure, $N_p$. In addition, $N_f$ and $N_i$ were defined as follows: $N_f$ is the number of cycles from the start of fatigue test to failure, whereas $N_i$ is the number of cycles from the start of fatigue test until the crack length reached 15 mm. The relationship between $N_f$, $N_i$ and $N_p$ can be shown as

$$N_f = N_i + N_p \tag{2}$$

$N_i$ is considered to be significantly depending on the dispersion of initial conditions such as residual stress and weld bead shape. In this study, $N_i$ was equivalent to 0.4–4.2 million cycles. Consequently, the difference in $N_p$ can be purely evaluated as the effect of repair.

Fig. 13 shows the fatigue test results arranged by the fatigue life $N_p$ after repair to failure. In all the series, the fatigue life $N_p$ was remarkably improved compared with the non-repaired series N. In series M, the fatigue life increased as the number of laminations increased. In particular, in series M5, the fatigue life

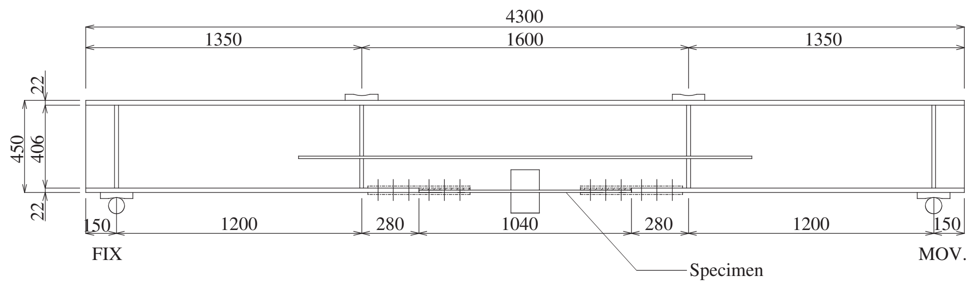


**Fig. 9.** Loading system.

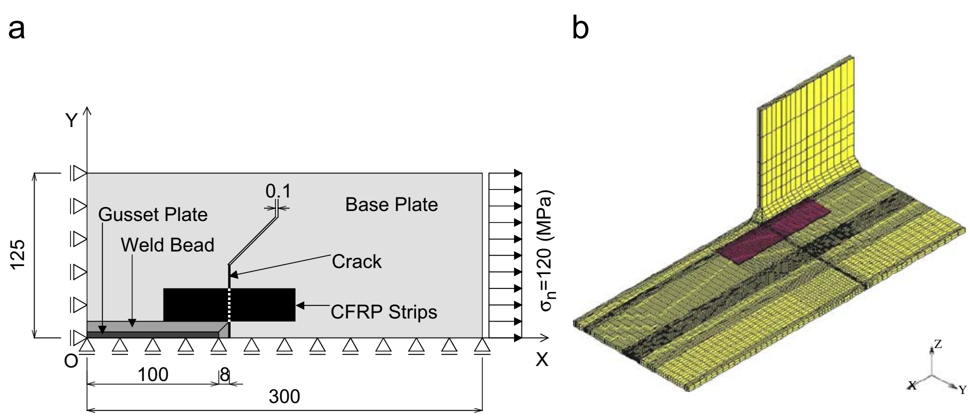


**Fig. 10.** Analytical model attached single-layered CFRP strip: (a) boundary conditions and (b) element division.

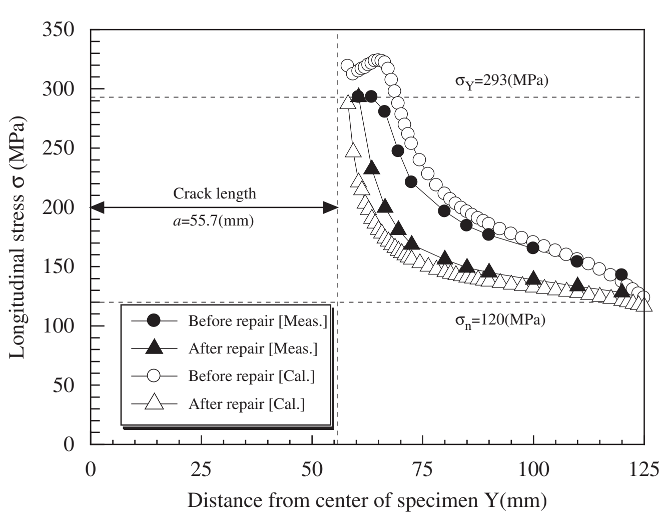


**Fig. 11.** Distribution of longitudinal stress.

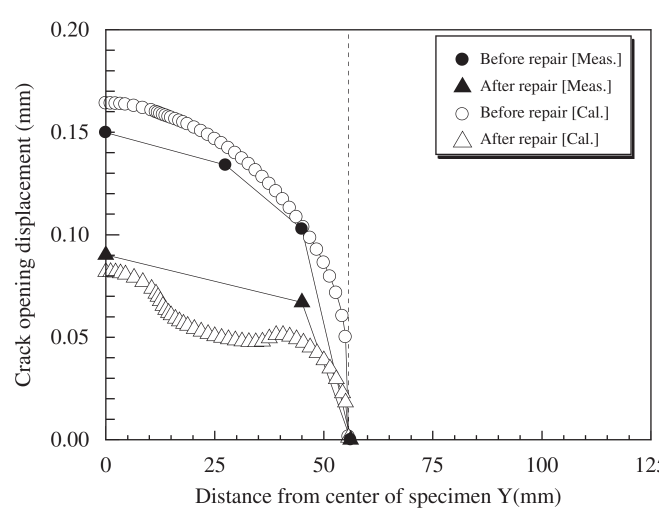


**Fig. 12.** Distribution of crack opening displacement.

improved remarkably in comparison with series N, indicating that a significant effect of repair was obtained. This is attributed to the fact that the crack opening was repaired by the high rigidity of multi-layered CFRP strips, and the opening displacement was sufficiently reduced. However, in this study, the fatigue limit was not obtained by series M5 within the stress range (64–114 MPa), although the fatigue life greatly exceeds 10 million cycles in the lowest stress range of 64 MPa.

Fig. 14 shows the relationship between the crack length and the number of cycles after repair in $\Delta\sigma_n = 64$ MPa. The crack lengths were measured within about 50–70 mm, using crack gages installed at the side of CFRP strips. Since crack lengths could not be measured in the bonding area of the CFRP strips, the dotted straight lines are shown in the figure. In series S and M, the fatigue life after repair is improved. The cracks progressed slowly in the bonding area of CFRP strips as shown by the dotted line in

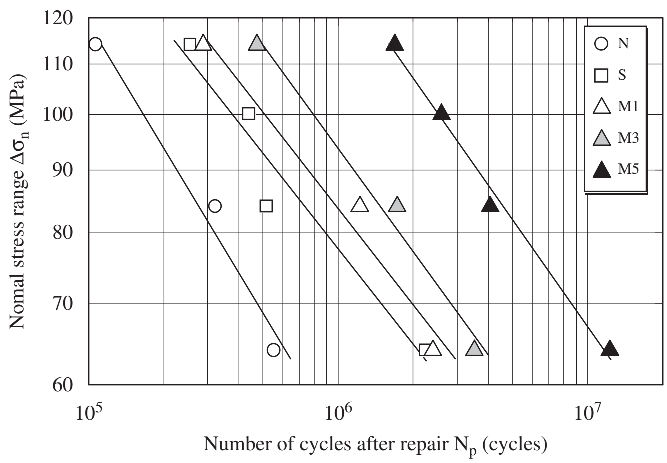


**Fig. 13.** $S$–$N_p$ diagram.

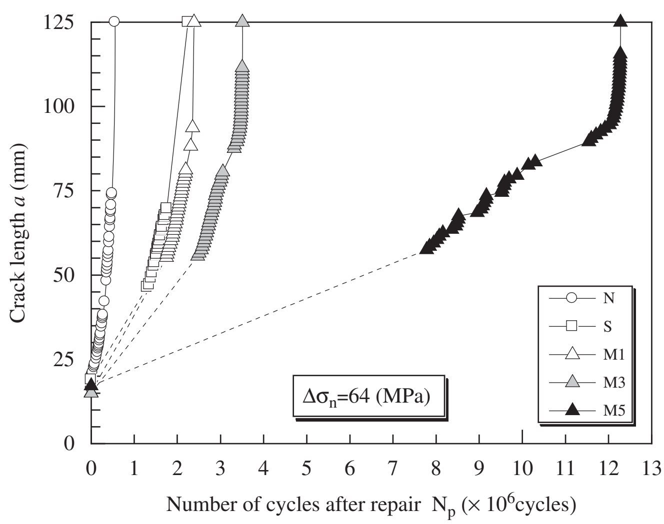


**Fig. 14.** Relationship between number of cycles after repair and crack length.

comparison with series N. In particular, in series M5, it was found that the crack progress was controlled effectively even after cracks crossed the bonding area. The crack propagated rapidly when crack length reached more than 95 mm (equivalent to about 75% of the overall width).

In series S, M1 and M3, CFRP strips did not debond within the bonding area. However, the cracks progressed gradually, and CFRP strips debonded when the crack length reached from 75 to 80 mm (a crack length ranging from 60% to 65% of the overall width). On the other hand, in series M5, CFRP strips debonded immediately before the specimen collapsed. In all specimens, debonding occurred in the interface of adhesive and steel plate.

In order to observe the bonding condition of CFRP strips, the fatigue test was stopped when the crack length reached approximately 100 mm (a crack length of about 80% of the overall width) in $\Delta\sigma_n = 100$ MPa. The specimen was removed from the loading system, and then cut off. Fig. 15 shows two macrosections in series M5. The multi-layered CFRP strips were very close and bonded well to the weld bead, though some partial defects remained.

**Table 3**
Experimental series of fatigue test.

| Series | Repair method | CFRP strip | |
|---|---|---|---|
| | | Single-layered part (mm) | Multi-layered part |
| N | Not repaired | – | – |
| S | Fig. 3(a) | 100 | – |
| M1 | Fig. 3(b) | 100 | 1-layer at 200 mm |
| M3 | Fig. 3(b) | 100 | 3-layer at 200 mm |
| M5 | Fig. 3(b) | 100 | 5-layer at 200 mm |

## 5. Combination of CFRP strips and drill-holes

### 5.1. Variation of repair methods and testing procedure

More effective repair methods were also investigated using combination of CFRP strips and drill-holes. A drill-hole is also called a stop-hole, and is often applied as a temporary repair method on site. Drill-holes are applied to reduce the stress concentration at the tips of cracks. Several combinations of CFRP strips and drill-holes were investigated by static loading tests and fatigue tests. The basic experimental procedure is the same as that mentioned above. In the specimen configuration, the width of the specimen was 300 mm in order to install two drill-holes of 25 mm diameter. Table 4 shows the material properties of steel, CFRP strips and epoxy resin adhesive.

Regarding variation in repair methods, four series of repair methods were examined as shown in Fig. 16 and Table 5. The cracked specimens were repaired when the crack progressed to 33 mm in length from the center towards the edge. The repair methods are described as follows:

(a) Series DH: repaired only by drill-holes.
(b) Series DHM: repaired with multi-layered CFRP strips (5 layers) and two drill-holes.
(c) Series DHS: repaired with single-layered CFRP strips bonded above two drill-holes.
(d) Series DHMS: repaired combining series DHM and DHS.

The diameter of drill-holes was 25 mm, which was similar to the diameter of a high-strength bolt. By installing drill-holes, the crack length was equivalent to 50 mm per side. The repair procedures and curing conditions are as mentioned above. In addition to these repair methods, the non-repaired series N was examined to give reference value.

Procedures of static and fatigue tests are the same as mentioned above. The nominal stress range $\Delta\sigma_n$ was 100 MPa in the fatigue test. Photograph 4 shows series DHMS as an example of repair methods. In addition, strain gages were installed on the surface of steel plate and CFRP strips, where the cracks would progress. The clip-type displacement transducers were installed in drill-holes and crack opening.

### 5.2. Static loading test results

Fig. 17 shows the longitudinal stress distribution of the steel plate in $\Delta\sigma_n = 100$ MPa (applied load: $\Delta P = 250$ kN) immediately after repair. The maximum stress was about five times the nominal tensile stress range $\Delta\sigma_n$ in series DH repaired only by drill-holes. In series DHS, DHS and DHMS, it was found that the maximum stress could be reduced by the combination of drill-holes and CFRP strips. In series DHMS, which was the most

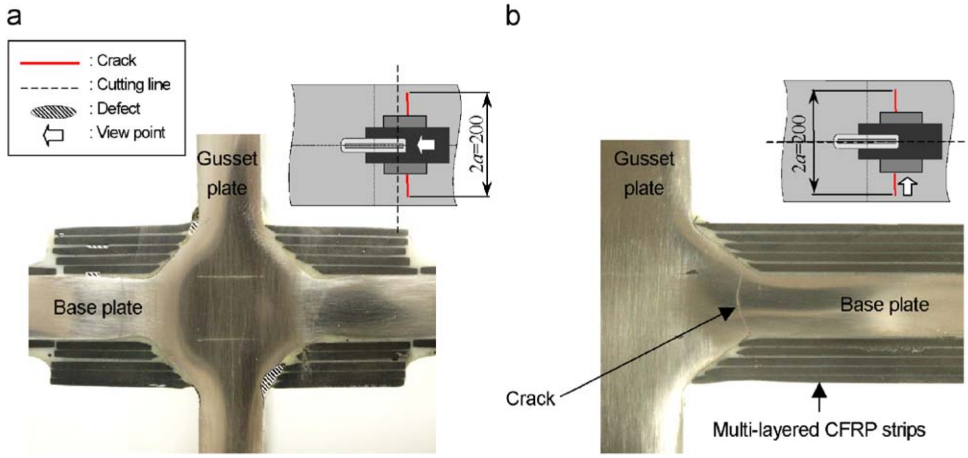


**Fig. 15.** Macrosections in series M5: (a) cross-sectional direction and (b) longitudinal direction.

**Table 4**
Mechanical properties of steel, CFRP strip and epoxy resin adhesive.

| | Steel plate (JIS SM400A) | CFRP strip | Epoxy resin adhesive |
|---|---|---|---|
| Yield point (MPa) | 285 | – | – |
| Tensile strength (MPa) | 443 | 2990 | 30 |
| Elongation (%) | 29 | 1.9 | – |
| Elastic modulus (GPa) | 206 | 172 | 1.5 |

effective repair, the maximum stress was reduced by about 50% compared with series DH.

Fig. 18 shows the longitudinal stress distribution on the CFRP strips. It can be said that the stress distribution in the multi-layered part of series DHMS was similar to that of series DHM. In the single-layered part of series DHMS, the stress distribution was lower than that of series DHS, it also showed that the stress on the steel plate was reduced as indicated above. Therefore, fatigue strength is expected to be the highest for series DHMS.

Fig. 19 shows the crack opening displacement (hereafter called the COD) in all series. In series DH, the COD after installing drill-holes (considered as 50 mm of the opening) obviously became larger compared with that before installing dill-holes (considered as 33 mm of the crack length). In series DHM, the COD could be remarkably reduced. On the other hand, in series DHS, the reduction of the COD at the center was small. In addition, the relationship between the applied load and the COD was almost linear.

### 5.3. Fatigue test results

Fig. 20 shows the $S$–$N_p$ diagram. $N_p$ was the fatigue life after repair (considered as 50 mm of the crack length) to failure, as defined by Eq. (2). The fatigue life $N_p$ of series DH and DHM were 1.6 and 5.0 times of the non-repaired series N, respectively. In series DHMS, where the fatigue test was continuing, $N_p$ was prolonged for 80 or more times compared to series N, and for 50 or more times compared to series DH. The sufficient effects of repair were confirmed. In addition, in series M5 with 250 mm wide specimen, the equivalent $N_p$ from 50 mm to failure was 1.15 million cycles. The fatigue life of series DHMS was greatly improved compared with that of series M5 without drill-holes.

More detail on fatigue tests is as follows. In series DHM, the multi-layered CFRP strips debonded on one side when $N_p$ was about 0.20 million cycles. The fatigue test was stopped because the crack generated again at the edge of drill-holes at about 0.33 million cycles. On the other hand, in series DHMS, the multi-layered CFRP strips debonded, when $N_p$ was about 0.47 million cycles on one side and about 4.30 million cycles on the other side, respectively. However, the debonding of single-layered CFRP strips and the recurrence of the crack at the edge of drill-holes were not observed even when $N_p$ reached to about 5.65 million cycles.

Although the stress concentration was reduced by installing drill-holes, the COD became larger. Consequently, the increase of the COD associated with installing drill-holes may have the influence on the debonding of CFRP strips.

## 6. Conclusion

For fatigue cracks initiated at the weld toe of web gusset joints, the repairs were performed using CFRP strips and epoxy resin adhesive, and the effects of repair on the bond strength and the fatigue durability were examined experimentally and analytically. The following conclusions were obtained:

(1) It was found that the proposed repair method greatly contributed to the increase of bond strength and the reduction of the opening displacement at the joint.
(2) The sufficient performance of adhesion joints was confirmed when the number of laminations of CFRP strips increased to five layers.
(3) The laminating of CFRP strips was found to be effective in preventing debonding and sharing axial force.
(4) It was confirmed that as the number of laminations of CFRP strips increases, the post-repair fatigue life improved considerably and that a sufficient effect of repair was acquired in the case of fivelayers.
(5) No fatigue limit was obtained from the discussed stress range. The proposed method was positioned as a first-aid repair to prolong the fatigue life, since no crack recurrence was prevented.

Moreover, regarding the more effective repair, some repair methods combining CFRP strips and drill-holes were also investigated experimentally. The repair method by combining

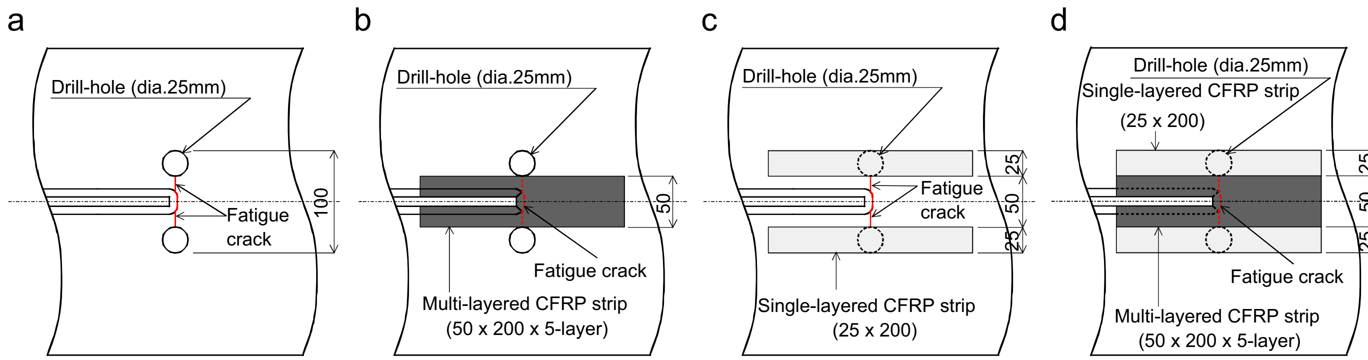


**Fig. 16.** Variation of repair methods: (a) series DH, (b) series DHM, (c) series DHS and (d) series DHMS.

**Table 5**
Experimental series in combination of CFRP strips and drill-holes.

| Series | Repair method | Drill-holes | CFRP strip | |
|---|---|---|---|---|
| | | | Single-layered part (mm) | Multi-layered part |
| N | Not repaired | Without | – | – |
| DH | Fig. 16(a) | 2-Dia.25 mm | – | – |
| DHS | Fig. 16(b) | 2-Dia.25 mm | 200 | – |
| DHM | Fig. 16(c) | 2-Dia.25 mm | – | 5-layer at 200 mm |
| DHMS | Fig. 16(d) | 2-Dia.25 mm | 200 | 5-layer at 200 mm |

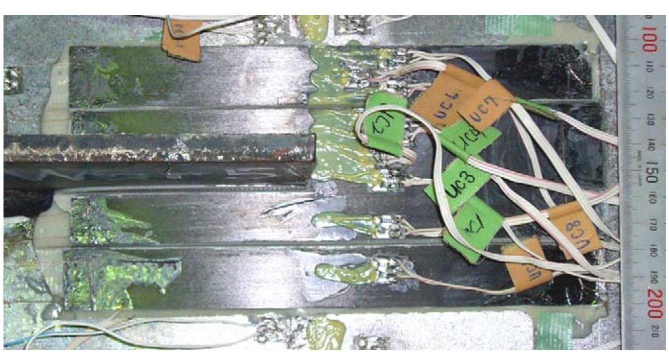

**Photograph 4.** Repair method in series DHMS.

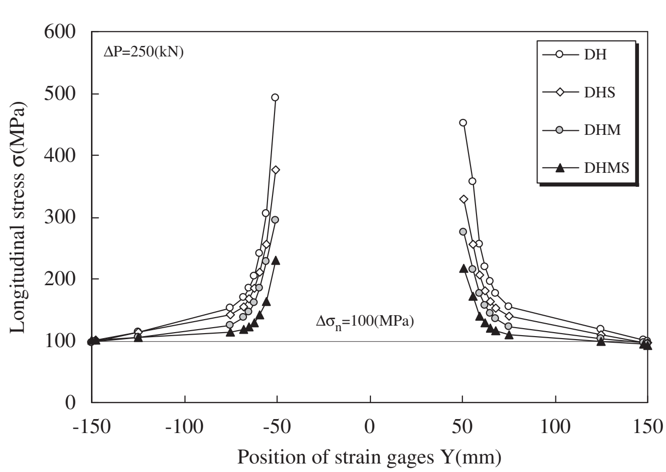


**Fig. 17.** Stress distribution of steel plate.

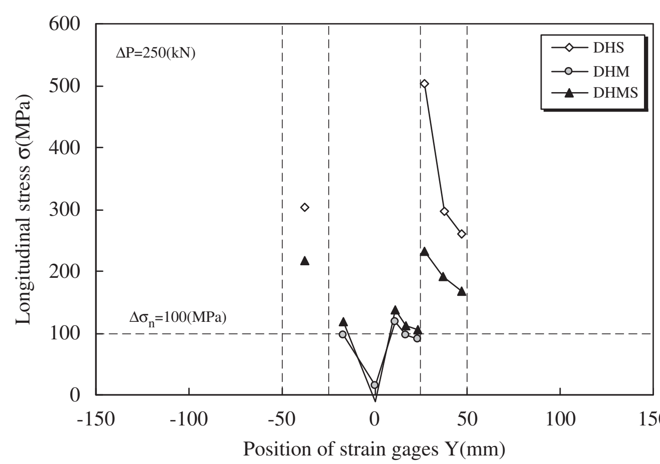


**Fig. 18.** Stress distribution of CFRP strips.

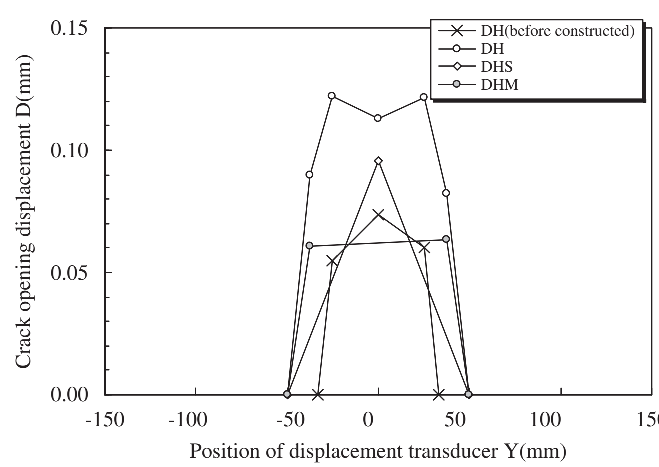


**Fig. 19.** Distribution of crack opening displacements.

CFRP strips and drill-holes was more effective compared with that without drill-holes.

It should be pointed out that the above conclusions were derived from the limited test data presented in this paper.

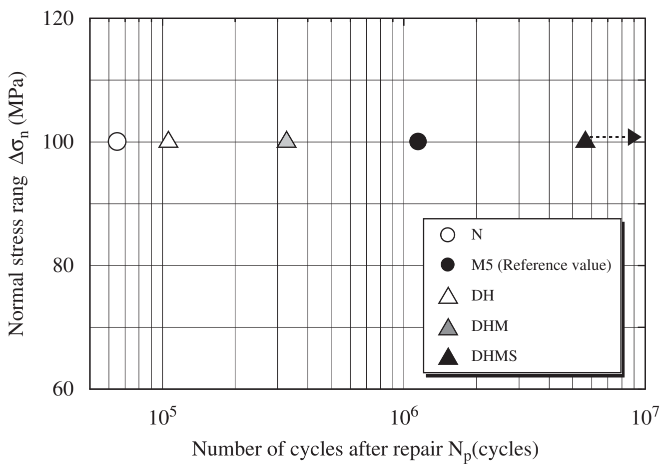


**Fig. 20.** $S$–$N_p$ diagram.

## References

[1] Japan Road Association. Guidelines for fatigue design of steel highway bridges. Tokyo: Maruzen Co., Ltd.; 2002 [in Japanese].

[2] Zhao X-L, Zhang L. State-of-the-art review on FRP strengthened steel structures. Engineering Structures 2007;29(8):1808–23.

[3] Hollaway LC, Cadei J. Progress in the technique of upgrading metallic structures with advanced polymer composites. Progress in Structural Engineering and Materials 2002;4(2):131–48.

[4] Smith ST. In: Proceedings of the first Asia-Pacific conference on FRP in structures—APFIS 2007, Hong Kong, 2007.

[5] Jiao H, Zhao XL. CFRP strengthened butt-welded very high strength (VHS) circular steel tubes. Thin-Walled Structures 2004;42(7):963–78.

[6] Miller TC, Chajes MJ, Mertz DR, Hastings JN. Strengthening of a steel bridge girder using CFRP plates. Journal of Bridge Engineering, ASCE 2001;6(6): 514–22.

[7] Bassetti A, Liechti P, Nussbaumer A. Fatigue resistance and repairs of riveted bridge members, fatigue design. Finland: Espoo; 1998. p. 535–46.

[8] Jones SC, Civjan SA. Application of fiber reinforced polymer overlays to extend steel fatigue life. Journal of Composites for Construction, ASCE 2003;7(4): 331–8.

[9] Tavakkolizadeh M, Saadatmanesh H. Fatigue strength of steel girders strengthened with carbon fiber reinforced polymer patch. Journal of Structural Engineering, ASCE 2003;129(2):186–96.

[10] Nakamura H, Yamasawa T, Maeda K, Doi T, Irube T, Takagi H, Suzuki H. Study on repair of steel members using CFRP strips. In: Proceedings of the 56th annual conference of JSCE, CD-ROM, 2001, 2 pages [in Japanese].

[11] Yamauchi T, Nakamura H, Maeda K, Suzuki H. Fatigue test on repair of steel members using CFRP strips. In: Proceedings of the 57th annual conference of JSCE. 2002. p. 1339–40 [in Japanese].

[12] Nakamura H, Moroi T, Suzuki H, Maeda K, Irube T. Repair of out-of-plane welded gusset joint using CFRP strips. Journal of Construction Steel, JSSC 2004;12:425–30 [in Japanese].

[13] Jiang W, Nakamura H, Suzuki H, Maeda K, Irube T. Experimental study on adhesion characteristics of steel plate and CFRP strips. Journal of Construction Steel, JSSC 2006;14:595–602 [in Japanese].